Clin Exp Metastasis (2006) 23:315–322
DOI 10.1007/s10585-006-9018-x

ORIGINAL PAPER

Visualization of nascent tumor angiogenesis in lung and liver metastasis by differential dual-color fluorescence imaging in nestin-linked-GFP mice

Yasuyuki Amoh · Michael Bouvet · Lingna Li · Kazuhiko Tsuji · A. R. Moossa · Kensei Katsuoka · Robert M. Hoffman

Received: 18 January 2006 / Accepted: 8 May 2006 / Published online: 30 November 2006

Abstract Nestin regulatory-element-driven green fluorescent protein (ND-GFP) transgenic mice highly express GFP in proliferating endothelial cells and nascent blood vessels. In the present study, we visualized angiogenesis in experimental lung and liver metastases by GFP imaging in the ND-GFP transgenic mice. The murine melanoma cell line, B16F10 expressing red fluorescent protein (RFP), was injected i.v. in ND-GFP mice. ND-GFP was highly expressed in proliferating nascent blood vessels in the tumors that developed in the lung after tail vein injection, and in the tumors that developed in the liver after portal vein injection of RFP-expressing melanoma cells. Liver metastasis and angiogenesis were imaged intravitally. Doxorubicin significantly decreased metastatic angiogenesis in the liver. These results demonstrate a new imageable model of angiogenesis in metastasis in the liver and the lung. This new model should enable further understanding of the onset of angiogenesis in metastasis and its effect on metastatic growth. The model will serve as a unique screen for inhibitors of angiogenesis of metastatic tumors. The fact that liver-metastasis angiogenesis can be imaged in the live animal enables real-time studies of the effect of angiogenesis inhibitors.

Keywords Metastasis · Angiogenesis · Fluorescent proteins · Imaging

Y. Amoh · L. Li · K. Tsuji · R. M. Hoffman (✉)
AntiCancer, Inc., 7917 Ostrow Street, San Diego, CA 92111, USA
e-mail: all@anticancer.com

K. Katsuoka · Y. Amoh
Department of Dermatology, Kitasato University School of Medicine, Sagamihara 228-8555, Japan

M. Bouvet · A. R. Moossa · Y. Amoh · K. Tsuji · R. M. Hoffman
Department of Surgery, University of California, San Diego, CA 92103, USA

K. Tsuji
Department of Pharmacology and Toxicology, Kyorin University School of Medicine, Shinkawa, Mitaka, Tokyo, Japan

Introduction

We previously reported that nestin, a marker for neural progenitor cells, is also selectively expressed in hair follicle stem cells [1, 2]. Transgenic mice with regulatory elements of the nestin gene driving expression of green fluorescent protein (ND-GFP mice) were used for these studies. We recently reported that many of the newly-formed vessels in the skin originate from hair-follicle cells during the anagen phase. These vessels are labeled with GFP in the transgenic mice expressing ND-GFP. The follicular origin of skin vessels is most evident after transplantion of ND-GFP-labeled follicles to unlabeled nude mice. After transplantation of the ND-GFP hair follicles, new fluorescent blood vessels originate from the labeled follicles. The vessels from the transplanted ND-GFP follicles respond to presumptive angiogenic signals from healing wounds [3].

We subsequently found that nestin is a marker for proliferating endothelial cells in the nascent blood vessels vascularizing the B16F10 melanoma expressing red fluorescent protein (RFP) transplanted subcutaneously in ND-GFP mice [4]. Immunohistochemical

staining showed that CD31 was expressed in the ND-GFP-expressing nascent blood vessels.

While much is known about angiogenesis in primary tumors, less is known about angiogenesis in metastatic tumors. In the present study, we demonstrate that angiogenesis of lung and liver metastatic tumors is visualized by GFP in the ND-GFP mice. Dual-color imaging enabled both the metastatic tumors, expressing RFP, and blood vessels expressing GFP, to be simultaneously visualized in the live animal. These results have particular importance for identifying and evaluating inhibitors of angiogenesis of metastatic tumors.

Materials and methods

ND-GFP transgenic mice [1]

Transgenic mice carrying GFP under the control of the nestin second-intron enhancer (ND-GFP mice) were originally obtained from Dr. G. Enikolopov (Cold Spring Harbor Laboratory, Cold Spring Harbor, NY).

RFP vector production [5]

The RFP (*DsRed-2*) gene (Clontech, Palo Alto, CA) was inserted in the retroviral-based mammalian expression vector pLNCX (Clontech) to form the pLNCX DsRed-2 vector. Production of retrovirus resulted from transfection of pLNCX DsRed-2 into PT67 packaging cells, which produce retroviral supernatants containing the *DSRed-2* gene. Briefly, PT67 cells were grown as monolayers in DMEM supplemented with 10% FCS (Gemini Biological Products, Calabasas, CA). Exponentially growing cells (in 10-cm dishes) were transfected with 10 μg expression vector using a LipofectAMINE Plus (Life Technologies, Grand Island, NY) protocol. Transfected cells were replated 48 h after transfection and 100 μg/ml G418 was added 7 h after transfection. Two days later, the medium was changed to 200 μg/ml G418. After 25 days of drug selection, surviving colonies were visualized under fluorescence microscopy and RFP-positive colonies were isolated. Several clones were selected and expanded into cell lines after virus titering on the 3T3 cell line.

RFP gene transduction of B16F10 melanoma tumor cell line [5]

For RFP gene transduction, 70% confluent rodent B16F10 melanoma cells were incubated with a 1:1 precipitated mixture of retroviral supernatants of PT67 cells and RPMI 1640 or other culture media (Life Technologies) containing 10% fetal bovine serum (Gemini Biological Products) for 72 h. Fresh medium was replenished at this time. Tumor cells were harvested with trypsin/EDTA and subcultured at a ratio of 1:15 into selective medium, which contained 50 μg/ml G418. To select brightly fluorescent cells, the level of G418 was increased to 800 μg/ml in a stepwise manner. Clones expressing RFP were isolated with cloning cylinders (Bel-Art Products, Pequannock, NJ) by trypsin/EDTA and were amplified and transferred by conventional culture methods in the absence of selective agent.

Lung metastasis model

ND-GFP transgenic mice, 6–8 weeks old were used. The mice were anesthetized with tribromoethanol (i.p. injection of 0.2 ml/10 g body weight of a 1.2% solution). B16F10-RFP cells were detached from the culture flask by a brief incubation with PBS containing 2 mM EDTA, suspended in RPMI 1640/10% FBS, washed, and resuspended in PBS. Fifty μl containing 2×10^6 B16F10-RFP cells per mouse were injected via the lateral tail vein with a 1 ml 27G1/2 latex-free syringe (Becton Dickinson). Animals were euthanized at day-14, and 28 and the lungs were removed for further studies. The lung samples were divided into two parts, one for direct observation by fluorescence microscopy and the other for frozen sections. For frozen sections, tumor samples were embedded in tissue-freeing embedding medium and frozen at –80°C overnight. Frozen sections 8 μm thick were cut with a Leica CM1850 cryostat, and were air-dried. Tissue samples taken at day-28 after injection were used to make frozen sections. Tissue was embedded in tissue-freezing medium and frozen at –80°C overnight. Frozen sections 10-μm thick were cut with a Leica CM1850 cryostat and were air-dried.

Liver metastasis model

ND-GFP transgenic mice, 6–8 weeks old, were used. The mice were anesthetized with tribromoethanol. B16F10-RFP cells were detached from the culture flask by a brief incubation with PBS containing 2 mM EDTA, suspended in RPMI 1640/10% FBS, washed, and resuspended in PBS. Fifty microliter containing 2×10^6 B16F10-RFP cells per mouse were injected via the portal vein with a 1 ml 27G1/2 latex-free syringe (Becton Dickinson). The liver was observed in live animals by opening the skin and peritoneum at days 5,

10, and 15 after injection under anesthesia. Tissue samples taken at day-15 after injection were used for frozen sections. Tissue was embedded in tissue-freezing medium and frozen at –80°C overnight. Frozen sections 10-μm thick were cut with a Leica CM1850 cryostat and were air-dried.

Anti-angiogenic efficacy of doxorubicin in the liver metastasis model

The mice were given daily intraperitoneal (i.p.) injections of 5 μg/g of doxorubicin or 0.9% NaCl solution (vehicle control) at days 5, 6, and 7 after injection of tumor cells. The doxorubicin regimen is described in our previous publications [3–5].

Fluorescence imaging of tissues [5]

Fluorescence microscopy was carried out using an Olympus IMT-2 inverted microscope equipped with a mercury lamp power supply. The microscope had a GFP filter set (Chroma Technology).

Whole-animal fluorescence imaging

The liver was imaged in live mice after opening the skin and peritoneum, at day-10 after portal-vein injection, under anesthesia. In order to observe liver metastasis in the live animal, after the skin and peritoneum were opened, a cover slip was placed on the liver surface. The animal was then placed in the Olympus OV100 Small Animal Imaging System (Olympus Corp., Tokyo, Japan) containing an MT-20 light source (Olympus Biosystems, Planegg, Germany) and DP70 CCD camera (Olympus Corp.). The optics of the OV100 fluorescence imaging system have been specially developed for macro as well as micro imaging with high light gathering capacity, and incorporate a unique combination of high numerical aperture and long working distance. Five individually optimized objective lenses, parcentered and parfocal, provide a 10^5-fold magnification range for seamless imaging of the entire body down to the subcellular level without disturbing the animal. The OV100 has the lenses mounted on an automated turret with a magnification range of 1.6×–16× and a field of view ranging from 6.9 mm to 0.69 mm. The optics and anti-reflective coatings ensure optimal imaging of multiplexed fluorescent reporters in small animals. High-resolution images were captured directly on a PC (Fujitsu Siemens, Munich, Germany). Images were processed for contrast and brightness and analyzed with the use of Paint Shop Pro 8 and Cell^R (Olympus Biosystems) [6]. We traced the ND-GFP expressing vessels with Adobe photoshop and calculated the total vessel length.

Immunohistochemical staining

CD31 was detected in frozen sections with the anti-rat immunoglobulin horseradish-peroxidase (HRP) detection kit (BD Pharmingen, San Diego, CA) following instructions from the manufacturer. The primary antibody was: CD31 mAb (1:50) (CBL1337) (Chemicon, Temecula, CA). Substrate-chromogen 3,3′-diaminobenzidine staining was used for antigen staining.

Statistical analysis

The experimental data are expressed as the mean ± SD. Statistical analysis was done using the two-tailed Student's *t*-test. All animal studies were conducted in accordance with the principles and procedures outlined in the National Institutes of Health Guide for the Care and Use of Animals under assurance number A3873-1.

Results and discussion

Visualizing ND-GFP angiogenesis of experimental lung metastasis

Mouse melanoma B16F10 cells, expressing RFP, were injected into the tail vein of ND-GFP transgenic mice. Immediately after tail vein injection, RFP-expressing tumor cells were visualized in ND-GFP expressing blood vessels in the walls of bronchioles, alveolar ducts, and alveolar sacs in frozen sections (Fig. 1a). At day-14, colonies of the RFP-positive tumor cells were visualized in thick sections of the lung. Nascent ND-GFP expressing vessels were visualized in the tumor (Fig. 1b). At day-28, the nascent ND-GFP-expressing vessels had increased in the growing tumor as visualized in thick sections of the lung (Fig. 1c).

Visualizing ND-GFP angiogenesis in experimental liver metastasis

Immediately after portal vein injection, RFP-expressing tumor cells were visualized in branches of the portal vein (Fig. 2a, b). At day-5, blood vessels were visualized by ND-GFP expression around the growing

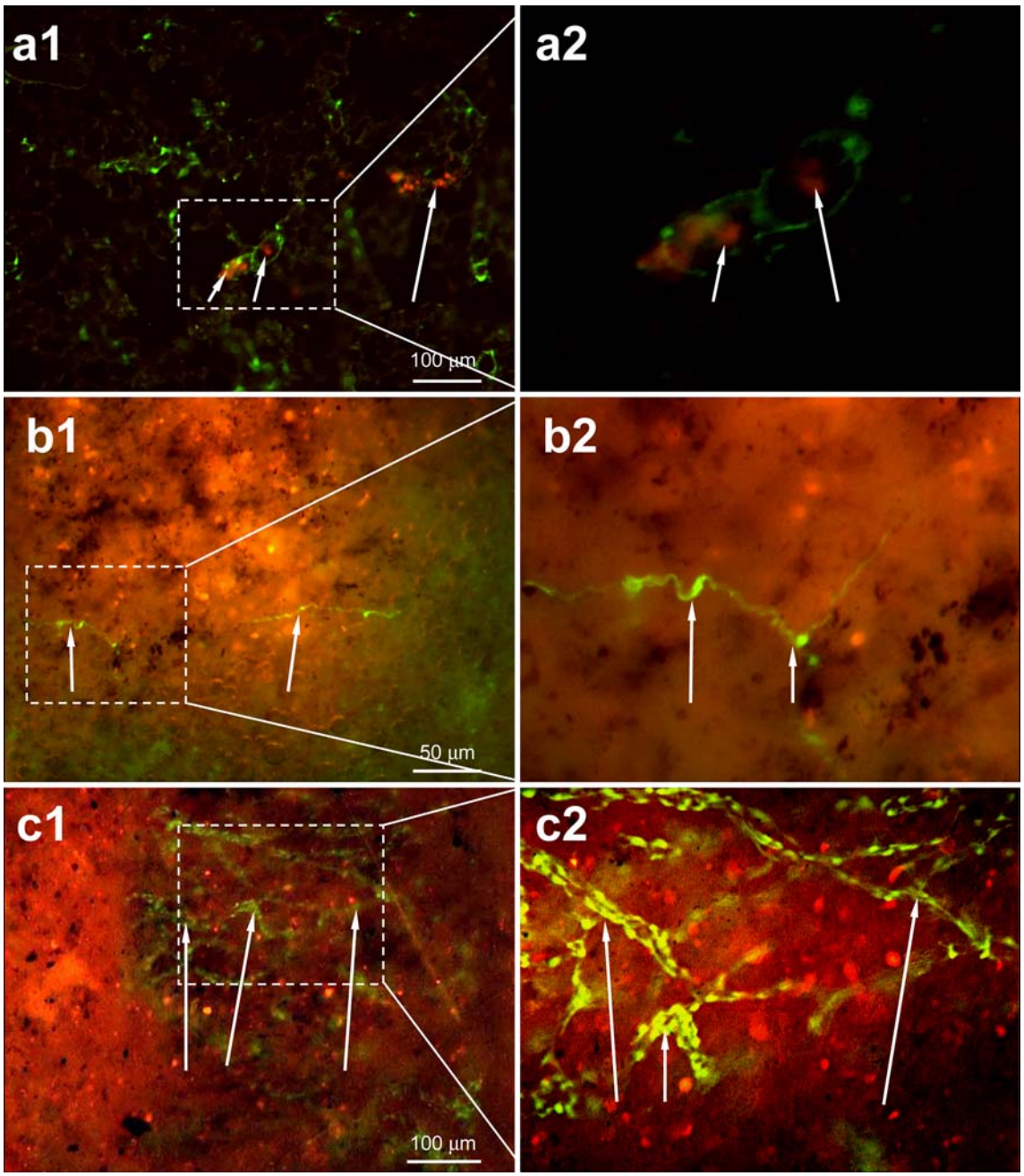

Fig. 1 Mouse melanoma (B16F10), expressing RFP, was injected into the tail vein of ND-GFP transgenic mice. (**a**) Immediately after tail vein injection, RFP-expressing tumor cells are visualized in ND-GFP expressing blood vessels in the walls of respiratory bronchioles, alveolar ducts, and alveolar sacs in the frozen section (white arrows). (**a2**) is a higher magnification of area of (**a1**) indicated by the white dashed box. (**b**) On day-14, colonies of the RFP-positive tumor cells could be visualized in a thick section of the lung. Nascent ND-GFP expressing vessels (white arrows) were growing into the tumor. (**b2**) is the higher magnification of the area of (**b1**) indicated by the white dashed box. (**c**) On day-28, the ND-GFP-expressing vessels (white arrows) were growing into the tumor seen in the thick section of the lung. (**c2**) is the higher magnification of area of (**c1**) indicated by the white dashed box

RFP-expressing tumor (Fig. 2c). At days-10 and -15, newly formed ND-GFP-expressing blood vessels were seen to increase in number and length in the RFP-expressing tumor (Fig. 2d, e). These observations were made intravitally.

CD31 expression in nascent ND-GFP expressing blood vessels, including those growing in tumors, was demonstrated in our previous publications [3–5], confirming that these ND-GFP structures were indeed blood vessels. In the current study, immunohistochemical

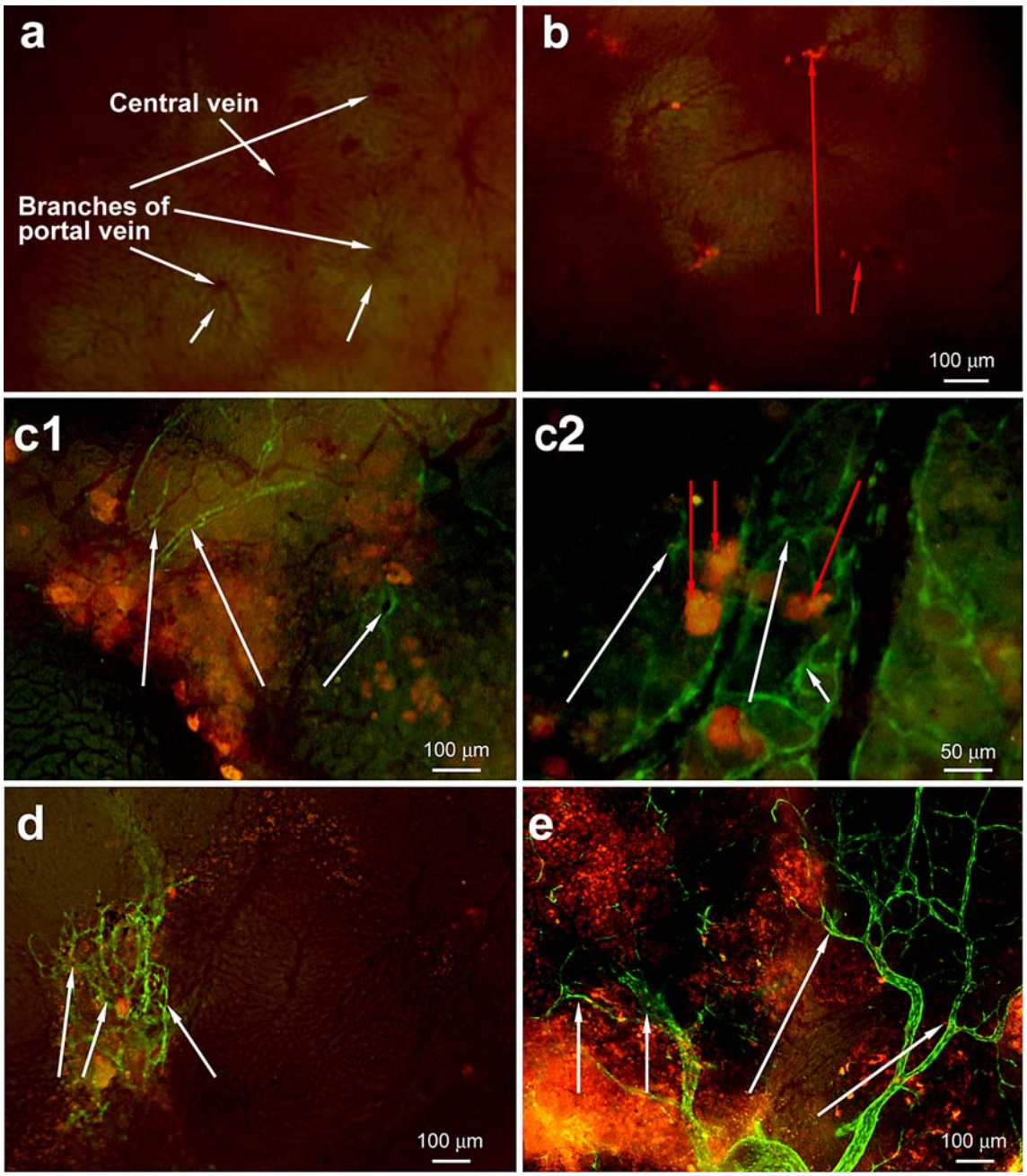

Fig. 2 (**a**) Normal liver of ND-GFP transgenic mice. The liver cells displayed autofluorescence due to bile. (**b**) Immediately after portal vein injection, RFP-expressing tumor cells were visualized in branches of the portal vein (red arrows). (**c1**) On day-5, pre-existing blood vessels visualized by ND-GFP expression around the growing RFP-expressing tumor cells (arrows). (**c2**) ND-GFP-expressing blood vessels begin to grow around the growing tumor cells (arrows). (**d**, **e**) At day-10 (**d**), and 15 (**e**), newly formed ND-GFP-expressing blood vessels were visualized growing in the RFP-expressing tumor (arrows)

staining showed that CD31 and nestin were colocalized in the blood vessels in the growing tumor. Frozen sections showing the ND-GFP blood vessels in the RFP-expressing B16F10 melanoma, metastasized to both liver and lung, were compared to sister sections stained for CD31 demonstrating colocalization of ND-GFP and CD31 in lung and liver metastasis (Fig. 3). We quantified the total length of ND-GFP expressing vessels, since these are the nascent vessels and most probably induced by the growing metastatic tumor colony (Fig. 4). We have previously observed that a normal lung has nestin-GFP-expressing blood vessels [5]. The tumor associated nestin-GFP vessels are identified, since the tumor is readily distinguished by

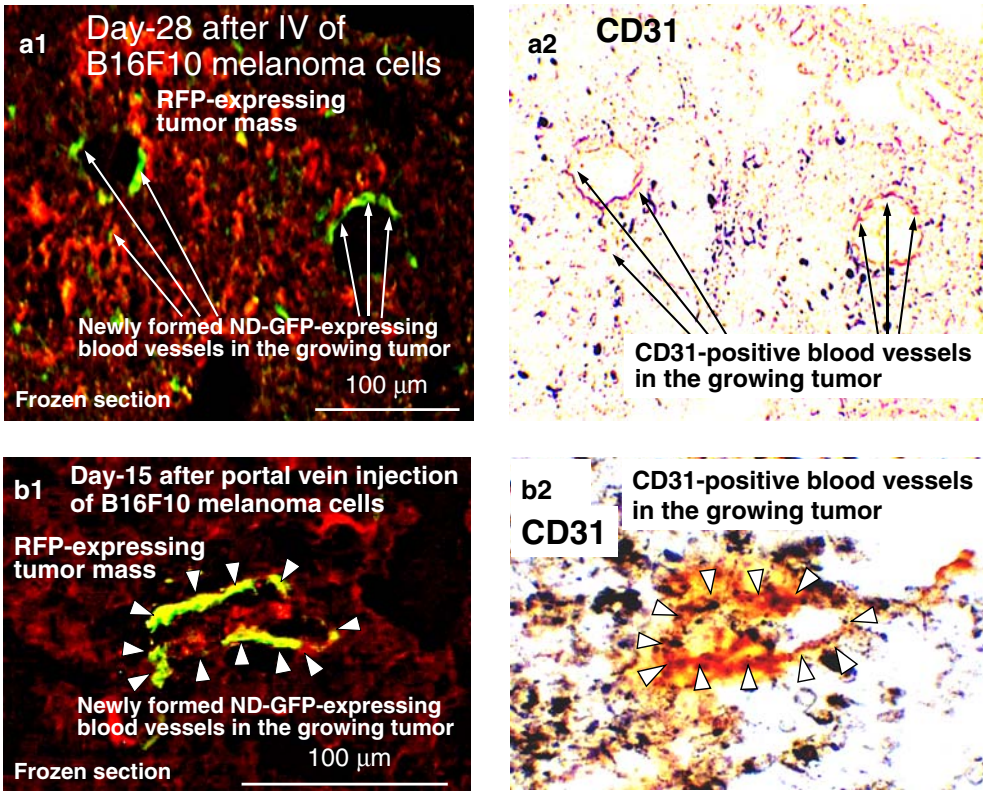

Fig. 3 Immunohistochemical staining of CD31. ND-GFP is visualized in blood vessels in the B16F10-RFP tumor in a frozen section of lung metastasis (**a**) and liver metastasis (**b**). Immunohistochemical staining in a sister frozen section shows CD31 colocalizing with ND-GFP blood vessels in the growing tumor

RFP expression. Future studies will determine functionality of the tumor-associated ND-GFP blood vessels.

Visualizing efficacy of doxorubicin on nascent angiogenesis on experimental liver metastasis

The ND-GFP-expressing nascent blood vessels were visualized to form a network in the growing tumor mass in the liver of untreated animals (Fig. 4a). The ND-GFP-expressing nascent blood vessels had many branches, and were connected to each other (Fig. 4a). The mice were given daily i.p. injections of doxorubicin. RFP-expressing tumor cells were growing only at the edge of the liver in the treated animals (Fig. 4b). The ND-GFP-expressing nascent blood vessels were sparse in the doxorubicin-treated mice (Fig. 4b). Mean vessel density in liver metastases was significantly decreased in mice treated with doxorubicin (Fig. 4c).

Angiogenesis is usually determined by immunohistochemical staining of tumor tissue using various antibodies specific for endothelial cells. The process of blood vessel formation is crucial to tumor development as a source of oxygen and nutrients. The blood vessels that form, which nourish a small tumor, enable the tumor to grow and eventually metastasize [7]. In the present study, proliferating endothelial cells during active angiogenesis were visualized in the growing metastatic tumor by ND-GFP expression. Simultaneously the tumor was visualized by RFP. The dual-color model provides a powerful and specific model to visualize nascent tumor angiogenesis simultaneously with metastatic tumor growth. Inhibition by doxorubicin of nascent angiogenesis in the metastatic tumors further demonstrates that angiogenesis is a critical target to prevent growth of metastatic tumors.

While there is an abundance of literature about angiogenesis in primary tumors, much less is known about angiogenesis in metastatic tumors. Recently, several investigators have noted that angiogenesis is important in lymph node metastases [8, 9]. Van den Eynden et al. attempted to quantify the level of hypoxia, endothelial cell proliferation, and angiogenesis in primary breast tumors and their axillary lymph node metastasis using immunohistochemical staining in archival tumor tissues. Their study suggested that growth of lymph node metastases is angiogenesis dependent. Likewise, Bjorndahl et al. [8] showed that blockage of VEGF-induced lymphangiogenesis in a mouse model of fibrosarcoma may provide a novel approach for prevention and treatment of lymphatic metastasis.

Angiogenesis also appears to be important in the development of visceral metastasis, including lung

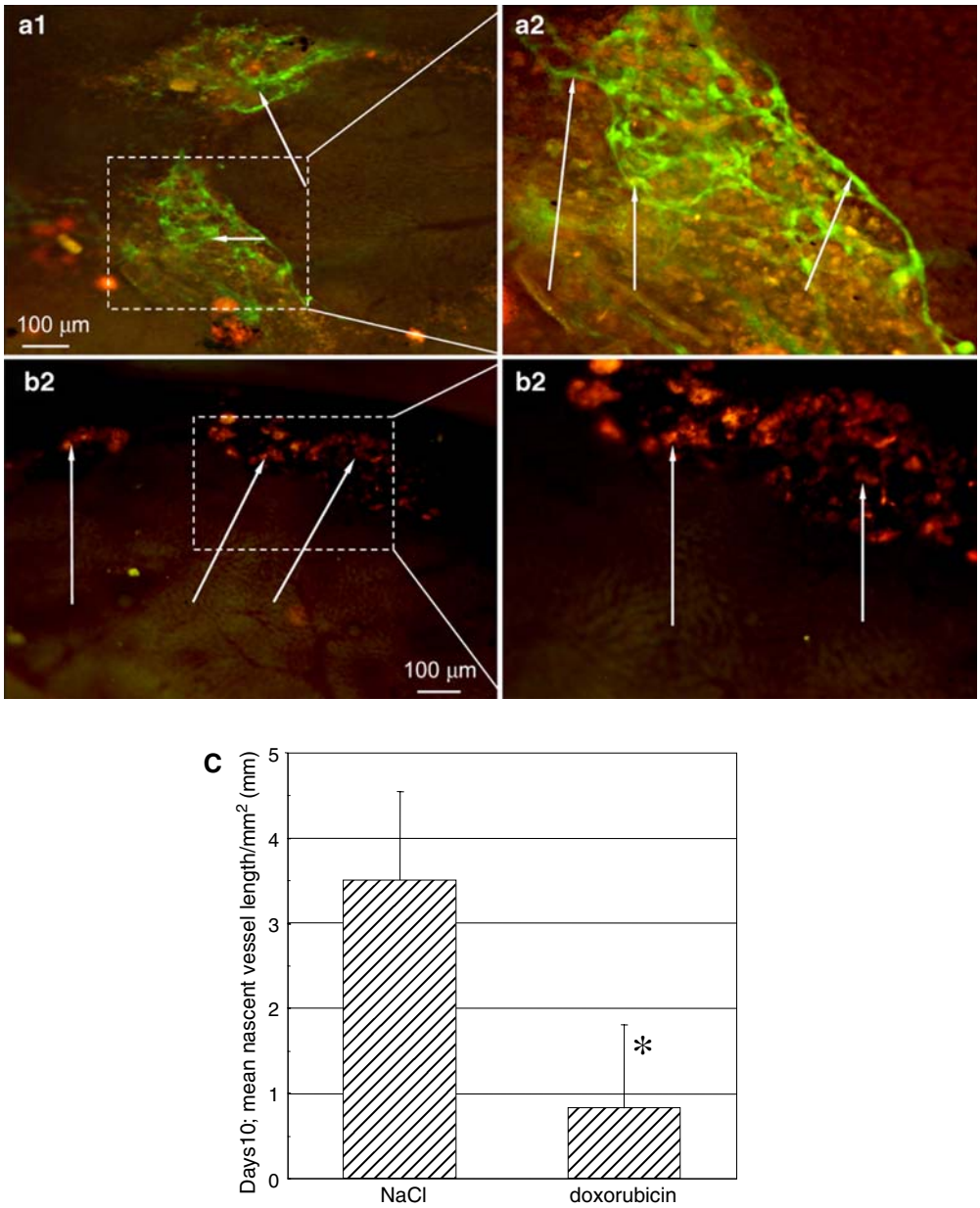

Fig. 4 (**a**, **b**) RFP-expressing tumor cells were injected via the portal vein of ND-GFP transgenic mice. The mice were given daily intraperitoneal (i.p.) injections of doxorubicin or 0.9% NaCl solution (vehicle control) on days 5, 6, and 7 after injection of tumor cells. The liver was directly observed in live animals with the Olympus OV100 Small Animal Imaging System on day-10 after injection. (**a**) The control mice were given daily i.p. injections of 0.9% NaCl solution. The ND-GFP-expressing nascent blood vessels formed a network in the growing tumor mass (white arrows). (**b**) The mice were given daily i.p. injections of doxorubicin. RFP-expressing tumor cells were growing only in the edge of the liver (arrows). The ND-GFP-expressing nascent blood vessels were very sparse. (**c**) Mean vessel density in the liver metastases was significantly decreased in mice treated with doxorubicin

and liver metastasis [10–12]. Using archival patient tumor specimens, Fukata et al. noted that levels of angiogenesis and expression of angiogenesis-related genes are prognostic for lung metastasis of renal carcinoma [10].

Takahashi and Mai [12] used antibodies against VEGF in a non-fluorescent orthotopic mouse model of colon cancer to inhibit liver metastasis. In that study, angiogenesis in metastatic liver tumors was quantified by vessel density and VEGF mRNA by in situ hybridization. In another study, Mi et al. found that multiple antiangiogenic pathways are necessary for the growth of hepatic metastases in a murine model of colon cancer [11].

The present study is a significant advance in that it enables simultaneous imaging of metastasis and angiogenesis in the live animal, including animals undergoing anti-tumor and anti-angiogenesis therapy. The study was enabled by multicolor fluorescent protein imaging [13].

Conclusions

In this study, we show that proliferating endothelial cells in experimental lung and liver metastasis express ND-GFP. Doxorubicin caused inhibition of the ND-GFP nascent blood vessels growth which inhibited melanoma cell growth in the liver as imaged in the live animal. These results demonstrate for the first time an imageable model of angiogenesis in visceral metastasis and the role of angiogenesis in metastasis formation.

Acknowledgements This study was supported in part by National Cancer Institute grant R21 CA109949-01 and American Cancer Society RSG-05-037-01-CCE (M. Bouvet) and National Cancer Institute grants CA099258, CA103563, and CA101600 (to AntiCancer, Inc.).

References

1. Li L, Mignone J, Yang M, Matic M, Penman S, Enikolopov G, Hoffman RM (2003) Nestin expression in hair follicle sheath progenitor cells. Proc Natl Acad Sci USA 100:9958–9961
2. Amoh Y, Li L, Katsuoka K, Penman S, Hoffman RM (2005) Multipotent nestin-positive, keratin-negative hair-follicle bulge stem cells can form neurons. Proc Natl Acad Sci USA 102:5530–5534
3. Amoh Y, Li L, Yang M, Moossa AR, Katsuoka K, Penman S, Hoffman RM (2004) Nascent blood vessels in the skin arise from nestin-expressing hair-follicle cells. Proc Natl Acad Sci USA 101:13291–13295
4. Amoh Y, Li L, Yang M, Jiang P, Moossa AR, Katsuoka K, Hoffman RM (2005) Hair follicle-derived blood vessels vascularize tumors in skin and are inhibited by Doxorubicin. Cancer Res 65:2337–2343
5. Amoh Y, Yang M, Li L, Reynoso J, Bouvet M, Moossa AR, Katsuoka K, Hoffman RM (2005) Nestin-linked green fluorescent protein transgenic nude mouse for imaging human tumor angiogenesis. Cancer Res 65:5352–5357
6. Tsuji K, Yamauchi K, Yang M, Jiang P, Bouvet M, Endo H, Kanai Y, Yamashita K, Moossa AR, Hoffman RM (2006) Dual-color imaging of nuclear-cytoplasmic dynamics, viability, and proliferation of cancer cells in the portal vein area. Cancer Res 66:303–306
7. Folkman J (2002) Role of angiogenesis in tumor growth and metastasis. Semin Oncol 29:15–18
8. Bjorndahl MA, Cao R, Burton JB, Brakenhielm E, Religa P, Galter D, Wu L, Cao Y (2005) Vascular endothelial growth factor-a promotes peritumoral lymphangiogenesis and lymphatic metastasis. Cancer Res 65:9261–9268
9. Van den Eynden GG, Van der Auwera I, Van Laere SJ, Colpaert CG, Turley H, Harris AL, van Dam P, Dirix LY, Vermeulen PB, Van Marck EA (2005) Angiogenesis and hypoxia in lymph node metastases is predicted by the angiogenesis and hypoxia in the primary tumour in patients with breast cancer. Br J Cancer 93:1128–1136
10. Fukata S, Inoue K, Kamada M, Kawada C, Furihata M, Ohtsuki Y, Shuin T (2005) Levels of angiogenesis and expression of angiogenesis-related genes are prognostic for organ-specific metastasis of renal cell carcinoma. Cancer 103:931–942
11. Mi J, Sarraf-Yazdi S, Zhang X, Cao Y, Dewhirst MW, Kontos CD, Li CY, Clary BM (2006) A comparison of antiangiogenic therapies for the prevention of liver metastases. J Surg Res 131:97–104
12. Takahashi Y, Mai M (2005) Antibody against vascular endothelial growth factor (VEGF) inhibits angiogenic switch and liver metastasis in orthotopic xenograft model with site-dependent expression of VEGF. J Exp Clin Cancer Res 24:237–243
13. Hoffman RM (2005) The multiple uses of fluorescent proteins to visualize cancer in vivo. Nat Rev Cancer 5:796–806